DEVELOPMENT OF TALL-3D TEST MATRIX FOR APROS CODE VALIDATION

I. Mickus, K. Kööp, M. Jeltsov, D. Grishchenko, P. Kudinov
Division of Nuclear Power Safety, Royal Institute of Technology (KTH)
Roslagstullsbacken 21, SE-10691, Stockholm, Sweden
mickus@kth.se; kaspar@safety.sci.kth.se; marti@safety.sci.kth.se; dmitry@safety.sci.kth.se; pkudinov@kth.se

J. Lappalainen
VTT Technical Research Centre of Finland
Vuorimiehentie 3, FI-02044 VTT, Espoo, Finland
jari.lappalainen@vtt.fi

ABSTRACT

APROS code is a multifunctional process simulator which combines System Thermal-Hydraulic (STH) capabilities with 1D/3D reactor core neutronics and full automation system modeling. It is applied for various tasks throughout the complete power plant life cycle including R&D, process and control engineering, and operator training. Currently APROS is being developed for evaluation of Generation IV conceptual designs using Lead-Bismuth Eutectic (LBE) alloy coolant.

TALL-3D facility has been built at KTH in order to provide validation data for standalone and coupled STH and Computational Fluid Dynamics (CFD) codes. The facility consists of sections with measured inlet and outlet conditions for separate effect and integral effect tests (SETs and IETs). The design is aimed at reducing experimental uncertainties and allowing full separation of code validation from model input calibration.

In this paper we present the development of experimental TALL-3D test matrix for comprehensive validation of APROS code. First, the representative separate effect and integral system response quantities (SRQs) are defined. Second, sources of uncertainties are identified and code sensitivity analysis is carried out to quantify the effects of code input uncertainties on the code prediction. Based on these results the test matrixes for calibration and validation experiments are determined in order to minimize the code input uncertainties. The applied methodology and the results are discussed in detail.

KEYWORDS

Generation IV, lead-bismuth eutectic, APROS, validation, dynamic process simulation

1. INTRODUCTION

Generation IV (Gen-IV) nuclear reactors are designed to use innovative cooling media such as liquid lead or liquid Lead-Bismuth Eutectic (LBE) alloy. The use of lead (or LBE) coolant yields a high natural circulation potential which is widely adopted in the Gen-IV reactor concepts for passive safety systems

such as the residual heat removal from the core. Correct modeling of the onset and stability of natural circulation is essential for system transient analysis and the design of the decay heat removal system [1].

Recently many System Thermal-Hydraulic (STH) codes, originally developed for LWR analysis, are being adapted for simulation of Gen-IV systems [2]. APROS code is a multifunctional process simulator which combines the STH capabilities with 1D/3D reactor core neutronics and full automation system modeling. It is applied for various tasks throughout the complete power plant life cycle including R&D, process and control engineering, and operator training. Currently APROS is being developed for evaluation of Gen-IV conceptual designs using LBE coolant. In this work we consider predictive code capabilities for the forced-to-natural circulation type transients, with special attention on the natural circulation development process and final characteristics of the steady-state circulation.

Each code extension requires validation against relevant experimental data. Previously, the TALL facility data was used for this purpose [3]. It was determined that qualitatively the behavior of the code agrees with the experiment, however the experimental uncertainties were too high to make quantitative conclusions. It was concluded that extensive analysis is necessary in order to develop the requirements for the design of the facility, validation and calibration test matrixes for successful quantitative code validation.

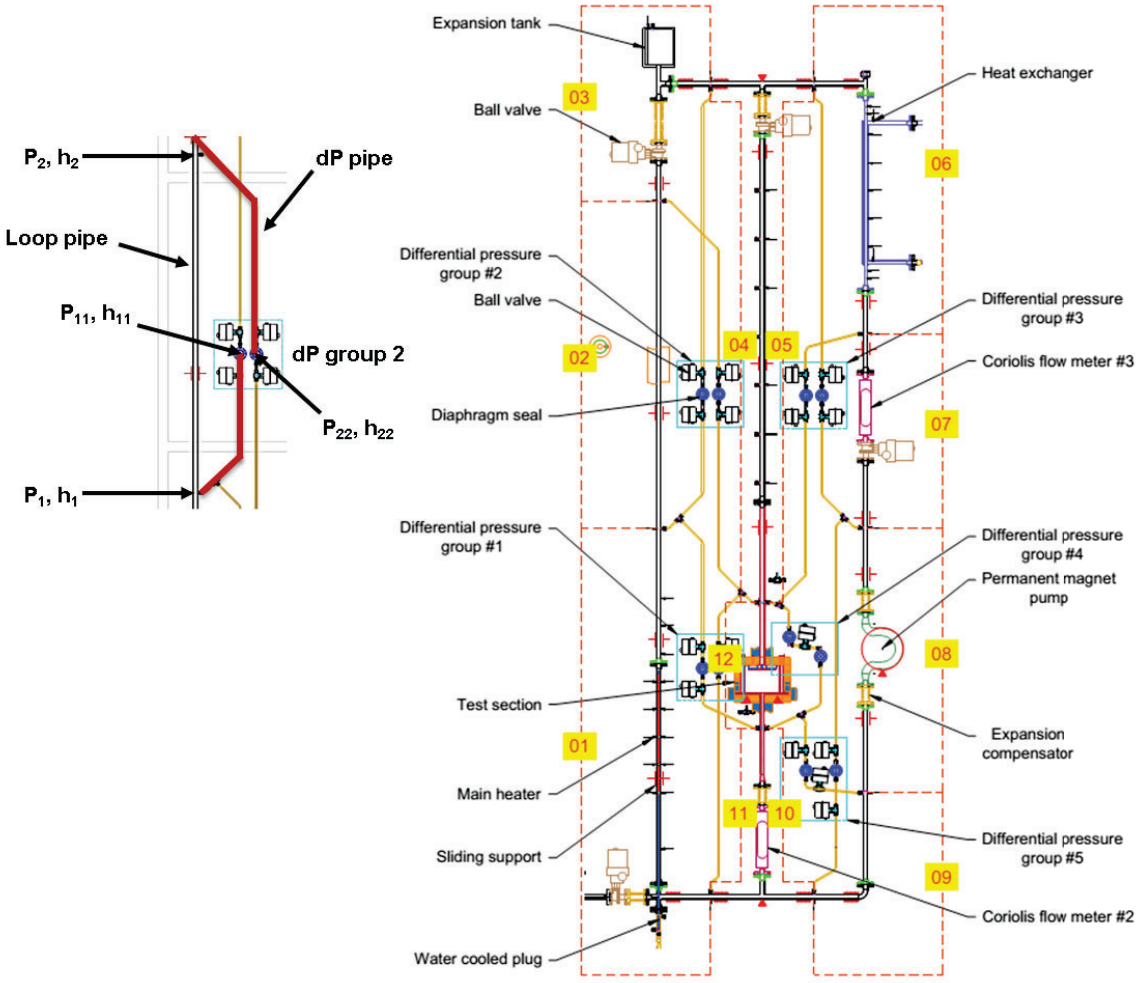

Figure 1: General layout of the TALL-3D facility and the group 2 of the differential pressure measurement system

The goal of this work is to develop and implement an approach for defining calibration and validation test matrixes and requirements for the measurements for the new TALL-3D facility. In order to achieve the goal we (i) define separate effect and integral system response quantities (SRQs); (ii) identify sources of uncertainties; (iii) carry out sensitivity analysis; (iv) define the test matrixes for calibration and validation experiments in order to minimize the influence of code input uncertainties and to enable quantitative validation of the code.

We briefly describe the TALL-3D facility in section 2; discuss our approach in section 3 and present some of the results in sections 4 and 5. Summary and outlook for the future work are given in section 6.

2. TALL-3D FACILITY

TALL-3D facility was designed and built at KTH primarily to provide validation data for standalone and coupled STH and CFD codes [4]. The primary loop is divided into 12 sections (see Table I and Figure 1) for which the flow temperatures and the pressure drop are measured with the aim of reducing the uncertainty in the inputs of computational codes by enabling section by section calibration.

The general layout of the facility is shown in Figure 1. The LBE (primary) loop of the facility consists of three vertical legs connected by two horizontal sections. The height of each vertical leg is 5.83 m and the distance between the adjacent legs is 0.74 m. The nominal piping inner diameter is 27.86 mm. Leg 1 with the Main Heater (MH) (on the left) consists of the pin-type electric heater (outer diameter 8.2 mm, heated length 870 mm, maximum power 27 kW) in the lower part, and the expansion tank at the top. Leg 2, the 3D leg (middle) contains the 3D test section. The upper part (two–thirds of the height) of the test section is equipped with two 7.5 kW rope heaters coiled jointly around the circumference of the test section. Leg 3 with the Heat Exchanger (HX) (on the right) contains the counter-current double-pipe heat exchanger placed at the top and the Electric Permanent Magnet (EPM) pump used for forced circulation of LBE. Each leg of the loop contains a ball valve enabling adjustment of the hydraulic resistances or a complete closure of the leg. The primary loop is thermally insulated with the exception of the EPM pump flow channel. The secondary side is used to remove heat from the primary loop during the tests and utilizes the Dowtherm heat transfer fluid.

Table I. Main loop sections and instrumentation

Section	Leg	Components	DP group	Inlet/Outlet TCs: TC[leg No.].[Elevation in mm]	Flow meter
1	1 (MH)	Lower left elbow and main heater	DP1	TC1.0000 / TC1.2641	FHX*-F3D**
2	1 (MH)	Vertical pipe on MH leg	DP2	TC1.2641 / TC1.4990	FHX-F3D
3	1 (MH)	Upper left elbow, ball valve, expansion compensator, expansion tank	DP2	TC1.4990 / TC1.5830	FHX-F3D
4	1-2 (MH-3D)	Upper left T-junction, ball valve	DP2	TC1.5830 / TC2.2111	FHX-F3D, F3D
5	3-2 (HX-3D)	Upper right T-junction, ball valve	DP3	TC3.5830 / TC2.2111	FHX,F3D
6	3 (HX)	Upper right elbow, Heat exchanger	DP3	TC3.5830 / TC3.4036	FHX
7	3 (HX)	Flow meter, and ball valve	DP3	TC3.4036 / TC3.2647	FHX
8	3 (HX)	EPM pump and 2 expansion compensators	DP5	TC3.2647 / TC3.0747	FHX
9	3 (HX)	Lower right elbow	DP5	TC3.0747 / TC3.0000	FHX
10	3-2 (HX-3D)	Lower right T-junction, flow meter	DP5	TC3.0000 / TC2.1211	FHX, F3D
11	1-2 (MH-3D)	Lower left T-junction, flow meter	DP1	TC1.0000 / TC2.1211	FHX-F3D, F3D
12	2 (3D)	3D test section	DP4	TC2.1211 / TC2.2111	F3D
* FHX – flow meter in the 3D leg; **F3D – flow meter in the HX leg					

Flow rates in HX and 3D legs are measured by Coriolis-type flow meters (flow meters 3 and 2 respectively). Flow rate in the MH leg is calculated from the mass balance. The LBE temperature is measured at 23 locations in the main loop. Additional thermocouples are installed in the LBE flow around the MH and in the 3D test section, on the main loop and differential pressure system piping and component walls, and in the thermal insulation. The differential pressure measurement system covers the whole primary. The differential pressures over 12 loop sections are measured by five differential pressure groups.

The design provides competing flow paths between the Main Heater (MH) leg and the leg with a 3D flow component – the 3D test section (3D leg). Such layout results in complex flow and temperature transients during natural circulation development.

3. APPROACH

3.1. Calibration and Validation

Not all parameters necessary for development of the code input (e.g. such as pressure and heat losses) are *directly* measured in the tests or provided in the experiment description. Therefore calibration of the code input parameters is a necessary step. Our approach aims to completely separate the input parameter calibration and subsequent code validation. This requires obtaining separate experimental data sets for calibration and validation. We aim to determine the values for uncertain input parameters only from the calibration experimental data. This means no subsequent model "tuning" to improve the agreement with the validation data.

The logical structure of the approach is shown in Figure 2. The process starts with the in-parallel development of the facility model in the code input and the experimental procedures to provide data for input model calibration and code validation. During the input model development step the uncertain input parameters and the corresponding ranges are defined. This depends on the modeling assumptions made by the code user and can be different for different conceptual realizations of the same physical reality. After model input development solution verification is performed. Solution verification is necessary to ensure that numerical uncertainties coming from the selection of node and time step sizes are lower than other uncertainty sources.

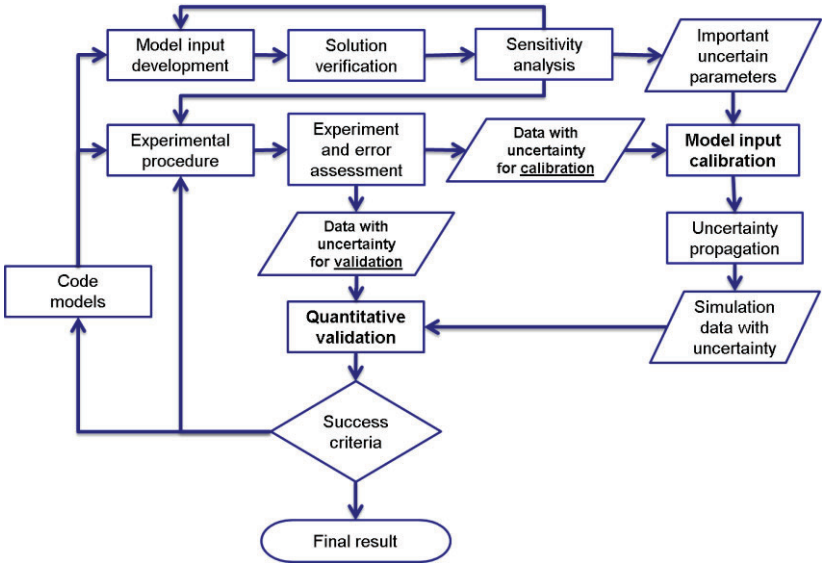

Figure 2: Quantitative validation process

Next, the sensitivity analysis for the identified uncertain model input parameters is performed. It allows ranking the model input parameters according to the influence on the simulation results and helps to gain a deeper insight about their effect to the model response. The results of the sensitivity analysis may indicate if the conceptual realization is flawed thus encouraging the user to rethink the conceptual realization and update the model. Feedback from sensitivity analysis is also provided to the experimental procedure with the goal to define the experimental conditions which would allow the greatest reduction of the model input uncertainty, by addressing the most influential uncertain parameters.

The uncertainty in the code prediction is reduced by first reducing the uncertainty in the most influential input parameters. This is achieved through model input calibration using dedicated experimental data. Since all experimentally measured values contain uncertainty, the calibration procedure would yield ranges for the uncertain input parameters. These would be narrower than the initial ones determined based on engineering judgment.

After obtaining the calibrated model the input uncertainties are propagated through the model to obtain the code response (SRQs) with the corresponding uncertainty. The result is then compared with the experimental validation dataset. The disagreement between the simulation and the experiment is quantified by applying a validation metric operator. Based on the results feedback can be provided to development of physical model and the experiment. For example, a decision to reduce code output uncertainty band further can be made, suggesting updates to the experimental equipment or procedures. The whole process can then be repeated iteratively by using the insights from previous iterations to improve the validation result.

3.2. TALL-3D Facility Model

The TALL-3D input model was developed following the same sub-division logic as in the actual facility. Each section (see Table I and Figure 1) of the primary loop is implemented separately in the model. The sections can be studied individually by applying section-wise boundary conditions or integrally as the full TALL-3D model. The secondary loop is modeled using flow and temperature boundary conditions at the inlet of the heat exchanger secondary side. The nodalization is done in a way that the actual position of a thermocouple corresponds to the middle of the node in the model.

We have defined several characteristic points for mass flow and temperature for the sensitivity analysis:

- Initial/Final mass flow rate values in the HX leg;
- Ratio between the initial mass flow rate values in the MH and 3D legs;
- Ratio between the final mass flow rate values in the MH and 3D legs;
- Ratio between the Maximum/Minimum peak transient mass flow rate and the initial mass flow rate values;
- Timing of the peak in the MH and 3D legs;
- Initial LBE temperature values at the MH, 3D section and HX inlet/outlet;
- Final LBE temperature values at the MH, 3D section and HX inlet/outlet;
- Ratio of initial to Maximum/Minimum peak transient temperature values at MH and 3D section outlets and HX inlet.

Uncertainty in prediction of the SRQs is affected by the uncertainty in the model input parameters. Several categories of model inputs can be distinguished: (i) geometry, (ii) material properties, (iii) initial and boundary conditions, and (iv) constitutive model parameters. The ranges used in the sensitivity study for each group of the input parameters are summarized in Table II. This is not an exhaustive list since total 94 uncertain parameters were defined considering independent parameter variation for each loop section.

Table II: Ranges for different groups uncertain input parameters used in the sensitivity analysis

Category	Parameter	Range*
Geometry	Thermal insulation thickness	Section specific
	Piping-insulation gap thickness	0.8 – 1.6 mm
Material properties	SS-316L thermal conductivity	±5 %
	SS-316L vol. heat capacity	±5 %
	Thermal insulation conductivity	±5 %
	Thermal insulation vol. heat capacity	±5 %
	Dowtherm fluid density	±5 %
	Dowtherm fluid heat capacity	±5 %
	Dowtherm fluid conductivity	±5 %
	Dowtherm fluid viscosity	±5 %
	Gap thermal conductivity	Air - steel
	Gap heat capacity	Air - steel
	Effective vol. heat capacity of uncertain heat structures	Section specific
	Effective thermal conductivity of uncertain heat structures	Section specific
Initial and boundary conditions	Main heater power	±1 %
	3D section heater power	±2 %
	Ambient temperature	25 – 45 °C
	Secondary coolant flow rate	±10 %
	Secondary coolant inlet temperature	±8 %
	Expansion tank pressure	1.1 – 1.5 bar
	Expansion tank temperature	200 – 400 °C
	EPM pump heat production in forced circulation	±30 %
Constitutive model parameters	Piping surface roughness	±100 %
	Local flow resistance coefficients	Section specific
*Percentage from a nominal value		

Model geometry was derived from CAD drawings which are based on measurements of the actual facility. General uncertainty in geometry such as the section-wise piping length is few millimeters and therefore small compared to the facility scale and thus was neglected. However, uncertainty is introduced when modeling geometrically complex objects as simple one-dimensional heat structures in cylindrical coordinates. Such objects as ball valves with actuators, flow meters, non-uniformity in thermal insulation, and the EPM pump flow channel were modeled preserving the heat exchange area between the structure and the LBE and defining “effective” parameters to account for heat losses and transient thermal inertia. The pre-heaters coiled around the main loop piping constitute a gap between the piping and the insulation. Both the thickness and the properties of this gap are uncertain. The thermal properties of the gap were modeled by defining the “gap material” with heat conductivity and capacity ranging from that of air to steel. Other material properties were implemented based on manufacturers’ specifications with the given uncertainties.

Initial and boundary conditions correspond to the powers of the heating elements, the characteristics (mass flow and inlet temperature) of the heat exchanger secondary side, the cover gas pressure and LBE temperature in the expansion tank, and the ambient temperature (additionally the section-wise inlet temperatures and LBE mass flow if a section-wise model is considered). The constitutive model parameters such as roughness of the surfaces in contact with the LBE and the local loss coefficients due to flow obstacles (e.g. bends, changes in flow area, T-junctions, MH supports, etc.) are uncertain as well. The values for the flow loss coefficients can vary significantly in literature as was summarized in [5]. Therefore initial selection of ranges for these parameters was based on previous experience and engineering judgment.

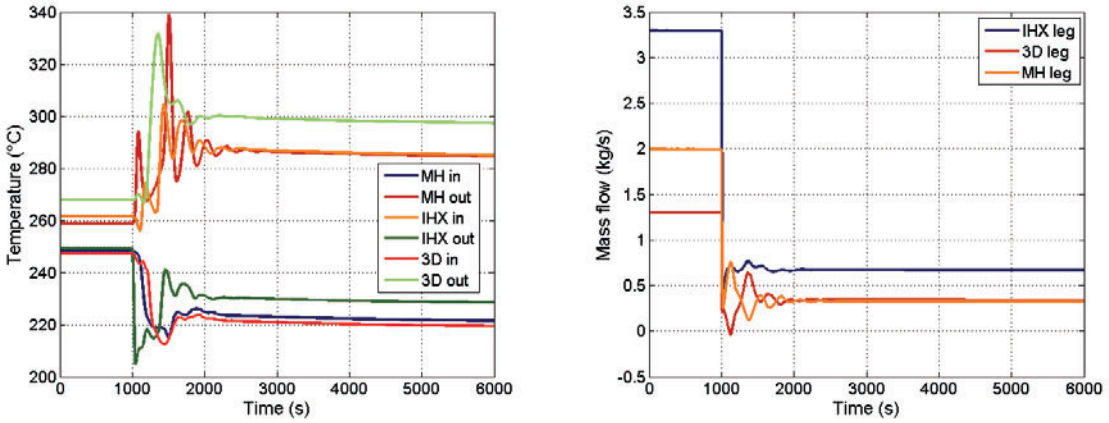

Figure 3: TALL-3D model (uncalibrated) transient response. LBE temperatures (left) and LBE mass flow rates (right)

Example of uncalibrated model response is shown in Figure 3. The pump was switched off after simulating a 1000 second forced circulation steady state. Transient to the natural circulation steady state followed after. The model predicts mass flow and temperature oscillations during the transient. Characteristic temperature peeks after reduction and subsequent recovery of the flow can be seen at the outlets of the MH and the 3D sections.

3.3. Sensitivity Analysis

We used the one-factor-at-a-time (OAT) method proposed by Morris for sensitivity analysis [6,7]. The method gives global sensitivity measures and allows determining the input parameters, which are negligible, have linear or additive effects, and have non-linear effects or are interacting with other input parameters. The value range of each input parameter is uniformly partitioned into p levels, constituting a p^k point grid at which the model evaluations take place. The model $y(\mathbf{x})$ is evaluated by generating r random samples (trajectories) from $\mathbf{x}$. The elementary effect corresponding to the input parameter i, for the j^{th} trajectory is computed as [8]:

$$d_i^{(j)} = \frac{y\left(\mathbf{x}^{(j)} + \Delta \mathbf{e}_i\right) - y\left(\mathbf{x}^{(j)}\right)}{\Delta} \tag{1}$$

Here $\mathbf{e}_i$ is the i^{th} coordinate vector in the input space (a vector of zeros but with a unit as its i^{th} component) and $\Delta = p/2(p-1)$. Then the mean μ, the modified mean μ^* and the standard deviation σ are computed for each input parameter i from the distribution of the corresponding elementary effects $d_i^{(j)}$ [8]:

$$\mu_i = \frac{1}{r}\sum_{j=1}^{r} d_i^{(j)}, \quad \mu_i^* = \frac{1}{r}\sum_{j=1}^{r} \left|d_i^{(j)}\right|, \quad \sigma_i = \sqrt{\frac{1}{r}\sum_{j=1}^{r}\left(d_i^{(j)} - \mu_i\right)^2}. \tag{2}$$

The mean and the modified mean describe the overall effect of an input parameter on the code output. The modified mean is used to avoid cancelation of the effects with varying signs. The standard deviation indicates non-linear effects or interactions.

The analysis was performed using the Dakota toolkit [8]. The toolkit was loosely coupled with the APROS code through Matlab script based interface for input pre-processing, simulation control and output post-processing. The required number of code runs (sample size) is equal to $r(k+1)$. Here k is the number of input parameters to be considered in the sensitivity study which in our case is equal to 94. As was demonstrated previously, r = 8 trajectories are sufficient to avoid wrongful rejection of an important parameter [9]. This resulted in 760 code executions.

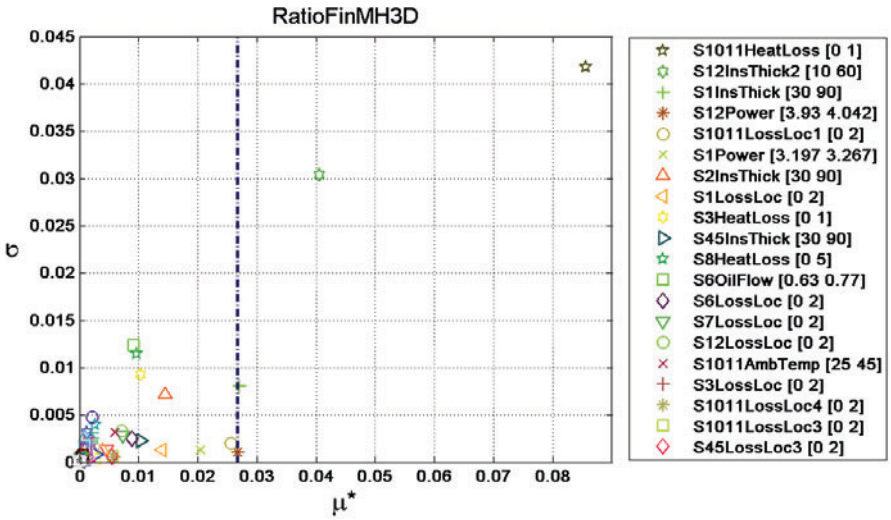

Figure 4. Ratio of end Final steady state natural circulation flow rates in the MH and 3D legs

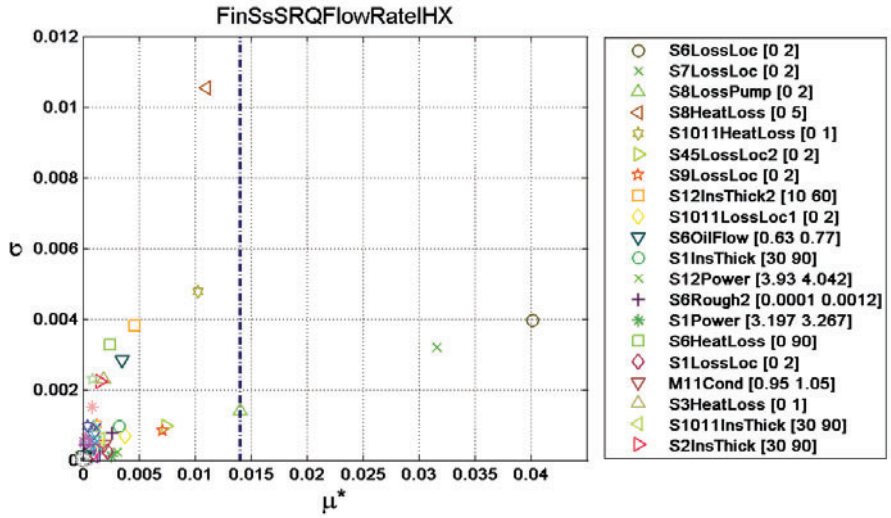

Figure 5. Final steady state natural circulation flow rate in the HX leg

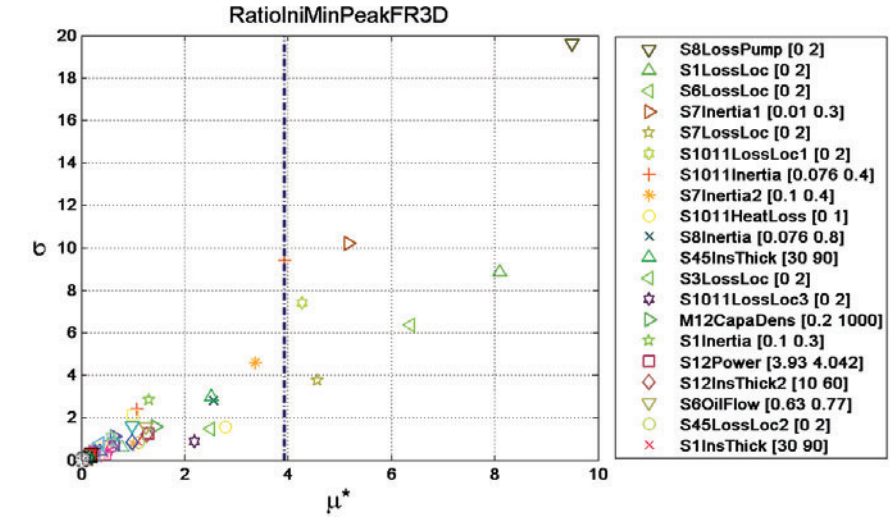

Figure 6. Ratio of minimum to initial transient peak flow rates in the 3D leg

4. SENSITIVITY ANALYSIS RESULTS

Selected results of the model sensitivity analysis are presented in Figure 4-Figure 9 as Morris diagrams. The dash-dot line indicates 50% of the cumulative modified mean for each SRQ. The legend entries are a combination of the loop section name (S1-S12), the uncertain parameter name, and the range of variation in brackets. The effective heat structure parameters and the local flow losses drive the variation in the studied SRQs. The properties of the structural materials (like piping steel and insulation) and some of the boundary conditions (e.g. ambient temperatures, or expansion tank parameters) are less important. Further on the influence of the individual input parameters is discussed for each Morris diagram.

The sensitivity of the ratio of LBE mass flow rates between the MH and 3D legs on the input parameters in the final natural circulation steady state is shown in Figure 4. The three most influential parameters are related with heat balances over the lower T-junction (with the LBE flow meter), the 3D test section and the MH section. High variation range for 3D section insulation thickness is motivated by installation specifics of the 3D heater. The heating element is not submerged in the LBE, but coiled around the periphery of the 3D test section. Therefore large part of the supplied power is lost through the insulation. Less important are the powers of the main and 3D section heaters and the local flow hydrodynamic losses in the bottom T-junction section and MH section. The dominating effect of parameters related to heat balance is observed due to the nature for the natural circulation flow which is driven by heating-up of the fluid and the resulting density differences between the loop sections.

The natural circulation flow rate in the HX leg is mostly sensitive to the hydrodynamic losses (see Figure 5). Here the local flow losses in the heat exchanger section, HX flow meter section, and EPM pump section have the largest effects. The next among the influential parameters are the heat losses through the EPM flow channel and in the 3D leg flow meter. The LBE flow rate in the HX leg is the highest in the loop, so the majority of the total loop hydraulic resistance is due to flow losses in this leg. The magnitude of natural circulation flow rate depends on the ratio between the hydrostatic forces, determined by heating and cooling, and the resistance to the flow. The parameters driving the flow resistance appear to be predominant in this case.

Sensitivity measures for the minimum transient peak flow rate in the 3D leg are shown in Figure 6. The SRQ was taken as a ratio between the transient peak and the initial flow rates to investigate the effect on the magnitude of the peak independently from the initial flow rate. Here a clear distinction of several parameters cannot be made. Combination of local flow losses and thermal inertia appears to dominate.

MH outlet temperature maximum transient peak SRQ has been scaled to the initial temperature to eliminate the effects of the parameters governing the initial steady state temperature at MH outlet (like the EPM pump heat generation). The magnitude of this peak depends on the residence time of the LBE in the MH section before flow recovery (see Figure 3, the timing of the peak corresponds to the timing of the first LBE flow rate recovery in the MH leg). The longer the residence time the larger the peak. The SRQ is influenced by a combination of local flow losses, heat losses and thermal inertia in the various sections of the loop (see Figure 7). The timing of this peak (see Figure 8) is mostly driven by thermal inertia (effective volumetric heat capacities of the loop structures and the piping-insulation gap) and heat losses in the 3D leg flow meter.

The final natural circulation steady state temperature at the MH outlet (see Figure 9) is mostly influenced by the coolant flow in the HX secondary side and the heat losses through the EPM pump flow channel.

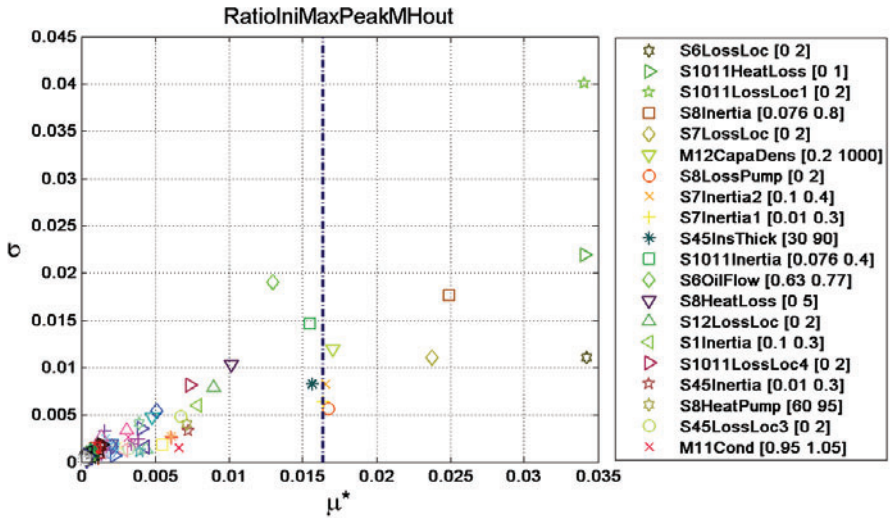

Figure 7. Ratio of initial to maximum transient temperature peak at MH outlet

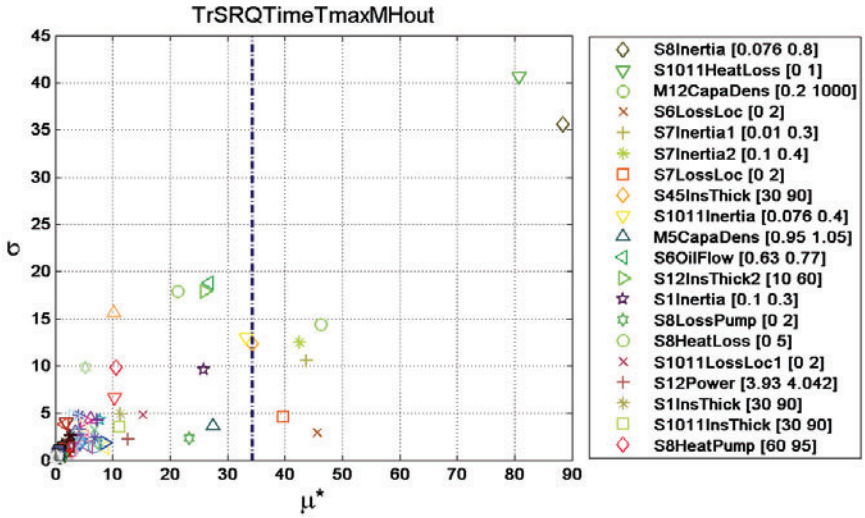

Figure 8. Timing of the maximum transient temperature peak at MH outlet

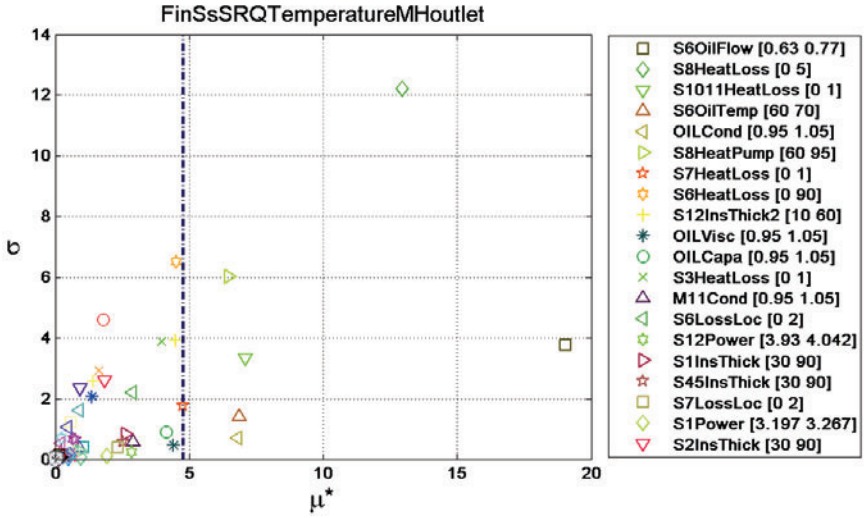

Figure 9. Final natural circulation steady state MH outlet temperature

5. TEST MATRIX REQUIREMENTS

5.1. Calibration tests

It is evident from the sensitivity analysis that to significantly minimize the model output uncertainty three main groups of uncertain input parameters must be calibrated (i) hydrodynamic losses (piping wall surface roughness and local flow loss coefficients); (ii) thermal losses (effective thermal resistances of the loop sections); and (iii) thermal inertia (effective heat capacities of the loop sections). The calibration should be done section by section in the model thus avoiding compensation of error when "tuning" several parameters at the same time.

Hydrodynamic losses can be determined from the pressure difference measurement over the facility sections. Assume we know the steady state pressure drop over some section from the experiment with the corresponding uncertainty $\Delta p_{l,e} \pm \delta\Delta p_{l,e}$. We want to obtain the same value in the model:

$$\Delta p_{l,e} \pm \delta\Delta p_{l,e} = \Delta p_{l,c} \pm \delta\Delta p_{l,c}. \tag{3}$$

Here $\Delta p_{l,c}$ is the steady state pressure drop predicted (calculated) for the same section and $\delta\Delta p_{l,c}$ is the uncertainty in prediction due the uncertainty in the measurement $\delta\Delta p_{l,e}$. The calculated pressure drop would have a general form of:

$$\Delta p_{l,c} \pm \delta\Delta p_{l,c} = f(k \pm \delta k, \lambda(Re \pm \delta Re, \varepsilon \pm \delta\varepsilon), \dot{m} \pm \delta\dot{m}, T) \tag{4}$$

where k is the local loss coefficient, λ is the friction factor and ε is the piping surface roughness. Let's consider ε first. In such case the Δp_l measurement should be taken at the loop section with no local flow obstructions (section 2) so k would be eliminated from eq. (4). By taking the LBE mass flow $\dot{m} \pm \delta\dot{m}$ from the experiment and assuming that the variation of viscosity due to uncertainty in the LBE temperature measurement is negligible (ignoring δT) we can vary the uncertain parameter in the model $\varepsilon \pm \delta\varepsilon$ to predict the experimental $\Delta p_{l,e} \pm \delta\Delta p_{l,e}$. This way the model is calibrated and the result is a range for the uncertain parameter ε. If a section contains local flow obstacles we would consider the full form of eq. (4) where $\varepsilon \pm \delta\varepsilon$ has been already calibrated from the pressure drop along section 2 (assuming piping surface roughness is the same for the entire loop). Considering combinations of $\varepsilon \pm \delta\varepsilon$ and $\dot{m} \pm \delta\dot{m}$ we can calibrate $k \pm \delta k$ in the model to obtain, section by section, the experimentally measured $\Delta p_{l,e} \pm \delta\Delta p_{l,e}$ for the remaining loop sections.

Due to the way how the pressure measurement system is implemented (see Figure 1), hydrostatic head corrections need to be applied to the pressure transducer readings. The transducer data channel provides the pressure difference value $\Delta p_m = p_{22} - p_{11}$. In case of isothermal conditions, the hydrostatic heads in the loop pipe and the pressure measurement system pipes would be equal ($h_{11}-h_1+h_2-h_{22}=h_2-h_1$, since $h_{11}=h_{22}$) and compensate for each other. So the value Δp_m would correspond to the actual hydrodynamic pressure loss. However, hydrostatic head of LBE is highly affected by temperature and such isothermal conditions are hard to realize in an experiment. Therefore correction is necessary to get pressures p_1 and p_2:

$$p_1 = p_{11} - g\int_{h_1}^{h_{11}} \rho(T)dh\,, \qquad p_2 = p_{22} + g\int_{h_{22}}^{h_2} \rho(T)dh \tag{5}$$

where T is the LBE temperature in the pressure measurement system pipes. Then the dynamic pressure loss would be obtained as:

$$\Delta p_{l,e} = p_2 - p_1 - \bar{\rho}g(h_2 - h_1) \tag{6}$$

Here $\bar{\rho}$ is the average LBE density for the LBE pipe section. The error in calculating $\Delta p_{l,e}$ thus largely depends on the error made in applying the hydrostatic head corrections. The temperature profile in the measurement system piping can be uncertain and largely influence the $\Delta p_{l,e}$ value. This uncertainty can

be reduced by taking measurements for the same loop section: first with LBE flow and second at stagnant flow conditions. The Δp_m reading at stagnant conditions should then correspond to the previously discussed correction due to the hydrostatic head differences. Both measurements should be taken in sequence to ensure the same thermal conditions. The lowest relative error in mass flow rate and pressure drop measurements would be obtained at high mass flow rates. This would also yield low temperature drops and thus low variation of LBE density over the LBE pipe sections. The temperature drops can be further reduced by performing the experiments at low LBE temperatures. Mass flow rate through a specific loop section can be increased by stopping the flow in either the MH or the 3D leg. To achieve such conditions the calibration tests for the pressure drops should be performed as described in Table III calibration test series 1.

Heat losses from the loop sections Q_e can be determined by calculating the steady state heat balance. Then the code solution:

$$Q_c \pm \delta Q_c = f(T_i \pm \delta T_i, \dot{m} \pm \delta \dot{m}, x \pm \delta x) = Q_e \pm \delta Q_e \tag{7}$$

where x is some code parameter governing the thermal resistance of the heat structures in the section model. Then taking the LBE mass flow $\dot{m} \pm \delta \dot{m}$ and the section inlet temperature $T_i \pm \delta T_i$ from the experiment, and optimizing the code solution $Q_c \pm \delta Q_c$ for $Q_e \pm \delta Q_e$ by adjusting x, the range $x \pm \delta x$ can be determined. In general, the heat losses are temperature dependent, and therefore the parameter x will also be temperature dependent. Therefore, the tests should be carried out at several temperature levels. The desired conditions for Q measurements are those where the effect is maximized, meaning high temperature drops over the loop sections. Such conditions are described in Table III as calibration test series 2. This would correspond to steady states with high LBE temperature and low LBE flow rates.

Thermal inertia I influences the transient temperature response and is commonly defined as:

$$I = \sqrt{\lambda \rho c_p} \tag{8}$$

Where λ is the effective thermal conductivity and ρc_p is the effective volumetric heat capacity. If the effective thermal conductivity has been previously assessed from the steady state heat balance measurements, the effective volumetric heat capacity can be assessed by studying temperature transient propagation through a loop section. The code response should be optimized to the experimental timing and temperature values by adjusting the effective volumetric heat capacity parameter for the section, and taking into account the uncertainties in mass flow ant temperature measurements. The effective parameter might be temperature dependent therefore the tests should be carried out at several temperature levels. When studying thermal inertia of the MH and the 3D sections, the respective heaters should be switched off. Such test conditions are described in Table III as calibration test series 3.

5.2. Validation tests

Validation tests commonly include separate effect tests (SETs) and integral effect tests (IETs). To perform validation against IETs, the code should first be validated against SETs. Opposite approach would complicate determination of which specific model implemented in the code is flawed. SETs require isolation of only one physical phenomenon of interest and high quality data for both the SRQ and the boundary conditions. Our ultimate goal is to simulate TALL-3D forced to natural circulation transients. Separate effects of flow hydrodynamic losses and surface to fluid heat transfer models should be assessed beforehand.

The section-wise TALL-3D facility design allows measuring the pressure drop over a 2.35 m long straight pipe section with no flow obstructions (section 2). The hydrodynamic flow losses in this section should thus occur only due to the wall surface friction. This allows performing a separate-effect test of the code's

Table III. Preliminary test matrix for model input calibration and code validation

Test series		Description	Test Conditions and Investigated Phenomena
Calibration tests	1	Temperature drop measurements over loop sections	**Test conditions:** EPM pump off, MH on, 3D heater on, all ball valves open, steady states at low LBE flow rates. **Investigated phenomenon:** section wise heat losses.
	2	Pressure drop measurements over loop sections	**Test conditions:** High LBE flow rates, EPM pump on, MH off, 3D heater off, pre-heaters on, steady state (MH or 3D ball valve closed). Isothermal conditions. Measurements of hydrostatic head off-set at stagnant flow. **Investigated phenomenon:** dynamic flow resistance.
	3	Temperature transient propagation through loop sections	**Test conditions:** Constant mass flow rate. MH off for S1 inertia investigation. 3D heater off for S12 inertia investigation. **Investigated phenomenon:** thermal inertia.
Validation tests	1	SETs of pressure drop over S2	**Test conditions:** Re numbers not covered in the calibration domain. Isothermal conditions. Measurements of hydrostatic head off-set at stagnant flow. **Investigated phenomenon:** wall surface friction.
	2	IETs - transients from forced to natural circulation	**Test conditions:** MH on, 3D section heater on. Various combinations of MH and 3D section powers. Secondary HX side boundary conditions as in calibration tests. **Investigated phenomenon:** natural circulation development with competing flow paths and driving heads.
	3	IETs - transients from forced to natural circulation	**Test conditions:** MH on, 3D section heater off. Various MH powers. Secondary HX side boundary conditions covered in calibration domain. **Investigated phenomenon:** natural circulation development with competing flow paths.

drag model for the LBE flow (see validation test series 1 in Table III). The drag SET data set should be obtained at LBE flow and LBE flow temperature boundary condition values outside the calibration domain (at different Re values) covering the operational range of the facility from forced to natural circulation flow. To keep the experimental uncertainty low, the same test procedures should be applied as was described for the calibration tests.

IETs cover conditions where multiple processes are involved and allow qualifying computational codes for the intended applications. Natural circulation development incorporates mutual feedback between thermal and flow phenomena and is important for safety assessment of heavy metal cooled reactors. IETs with both MH and 3D section heaters on provide competing driving forces for LBE natural circulation and result in transients with complex LBE mass flow and temperature oscillations (validation test series 2 in Table III). Yet, fluid stratification in the 3D test section and the subsequent mixing yield 3D effects which, if sufficiently strong, an STH code should not be able to predict. Therefore separate STH code validation IETs with elimination of the 3D effects by switching off the 3D section heater could be performed (validation test series 3 in Table III). Since the HX secondary side boundary conditions are large contributors to the overall uncertainty, the validation IETs should be performed with these boundary conditions covered in the calibration domain.

6. SUMMARY AND OUTLOOK

In this paper we have discussed the approach to validation of APROS code's LBE flow simulation capabilities against TALL-3D experimental data where the code validation is separated from the model input calibration. For this purpose two separate sets of experimental data are necessary – the calibration data set and the validation data set. We have performed sensitivity analysis and determined that parameters governing heat losses, dynamic pressure losses and thermal inertia are the most influential model input parameters for the selected computational SRQs in the forced to natural circulation type transients. Based on these results we have discussed the section by section calibration approach with the corresponding experimental conditions and proposed three series of calibration tests. These tests would allow reducing the model input uncertainty before code validation. Further we have proposed the SET series for validation of the surface friction model and two series of natural circulation development validation IETs.

The work is continued by assessing the currently available TALL-3D experimental data. Confidence in the currently obtained data and the related experimental errors is being evaluated. Code input calibration and propagation of input uncertainties will be performed as the next steps.

ACKNOWLEDGMENTS

This work has been supported by Fortum Oyj.

REFERENCES

1. X. Cheng, A. Batta, G. Bandini, F. Roelofs, K. Van Tichelen, A. Gerschenfelde, M. Prasser, A. Papukchiev, U. Hampelh, W.M. Ma, "European activities on crosscutting thermal-hydraulic phenomena for innovative nuclear systems," *Nucl. Eng. Des.* (article in press) (2014).
2. G. Bandini, M. Polidori, A. Gerschenfeld, D. Pialla, S. Li, W.M. Ma, P. Kudinov, M. Jeltsov, K. Kööp, K. Huberd, X. Cheng, C. Bruzzese, A.G. Class, D.P. Prill, A. Papukchiev, C. Geffray, R. Macian-Juan, L. Maas, "Assessment of systems codes and their coupling with CFD codes in thermal–hydraulic applications to innovative reactors," *Nucl. Eng. Des.* **281**, pp. 22-38 (2015).
3. I. Mickus, J. Lappalainen, P. Kudinov, "Validation of APROS Code Against Experimental Data from a Lead-Bismuth Eutectic Thermal-Hydraulic Loop," *Proceedings of ICAPP 2015*, Nice (France), Paper 15178, May 03-06 (2015).
4. D. Grishchenko, M. Jeltsov, K. Kööp, A. Karbojian, W. Villanueva, P. Kudinov, "The TALL-3D Facility Design and Commissioning Tests for Validation of Coupled STH and CFD Codes," *Nucl. Eng. Des.* (article in press) (2015).
5. W. Jaeger, V.H. Sánchez Espinoza, "Uncertainty and Sensitivity Analysis for the HELIOS Loop within the LACANES Benchmark," *Int. J Energ. Pow. Eng.* **5**, pp. 515-524 (2011).
6. M. D. Morris, "Factorial Sampling Plans for Preliminary Computational Experiments," *Technometrics*, **33**(2), pp. 161-174 (1991).
7. A. Saltelli, S. Tarantola, F. Campolongo, M. Ratto, *Sensitivity Analysis in Practice*, pp. 91-108, John Wiley & Sons Ltd, West Sussex, England (2004).
8. Adams, B.M., Bauman, L.E., Bohnhoff, W.J., Dalbey, K.R., Ebeida, M.S., Eddy, J.P., Eldred, M.S., Hough, P.D., Hu, K.T., Jakeman, J.D., Swiler, L.P., and Vigil, D.M., "DAKOTA, A Multilevel Parallel Object-Oriented Framework for Design Optimization, Parameter Estimation, Uncertainty Quantification, and Sensitivity Analysis: Version 5.4 User's Manual," Sandia Technical Report SAND2010-2183 (2009).
9. C. Geffray, R. Macian-Juán, "A Study of Different Approaches for Multi-Scale Sensitivity Analysis of the TALL-3D Experiment using Thermal-Hydraulic Computer Codes," *The 10th International Topical Meeting on Nuclear Thermal-Hydraulics, Operation and Safety (NUTHOS-10)*, Okinawa, Japan, Paper 1052, December 14-18 (2014).